



Physicochemical characterization of C-phycoyanin from *Plectonema* sp. and elucidation of its bioactive potential through in silico approach

Arbab Husain¹, Alvina Farooqui^{2*}, Afreen Khanam¹, Shubham Sharma², Sadaf Mahfooz¹, Adeeba Shamim¹, Firoz Akhter³, Abdulrahman A. Alatar⁴, Mohammad Faisal⁴, Saheem Ahmad^{5*}

¹IIRC-1, Laboratory of Glycation Biology and Metabolic Disorder, Department of Biosciences, Faculty of Sciences, Integral University, Lucknow-226026, India

²Department of Bioengineering, Faculty of Engineering, Integral University, Lucknow-226 026, India

³Department of Biomedical Engineering, Stony Brook University, New York, USA

⁴Department of Botany & Microbiology, College of Science, King Saud University, P.O. Box 2455, Riyadh 11451, Saudi Arabia

⁵Department of Medical Laboratory Sciences, College of Applied Medical Sciences, University of Hail, Kingdom of Saudi Arabia

ARTICLE INFO

Original paper

Article history:

Received: July 29, 2021

Accepted: November 01, 2021

Published: December 01, 2021

Keywords:

Cyanobacterium; C-phycoyanin; *Plectonema* sp.; Antioxidant; Antidiabetic

ABSTRACT

C-phycoyanin (C-PC), the integral blue-green algae (BGA) constituent has been substantially delineated for its biological attributes. Numerous reports have illustrated differential extraction and purification techniques for C-PC, however, there exists paucity in a broadly accepted process of its isolation. In the present study, we reported a highly selective C-PC purification and characterization method from nontoxic, filamentous and non-heterocystous cyanobacterium *Plectonema* sp. C-PC was extracted by freeze-thawing, desalted and purified using ion-exchange chromatography. The purity of C-PC along with its concentration was found to be 4.12 and 245 µg/ml respectively. Comparative characterization of standard and purified C-PC was performed using diverse spectroscopic techniques namely Ultra Violet-visible, fluorescence spectroscopy and Fourier transform infrared (FT-IR). Sharp peaks at 620 nm and 350 nm with UV-visible and FT-IR spectroscopy respectively, confirmed amide I bands at around 1638 cm⁻¹ (C=O stretching) whereas circular dichroism (CD) spectra exhibited α -helix content of secondary structure of standard 80.59% and 84.59% of column purified C-PC. SDS-PAGE exhibited two bands of α and β subunits 17 and 19 kDa respectively. HPLC evaluation of purified C-PC also indicated a close resemblance of retention peak time (1.465 min, 1.234 min, 1.097 min and 0.905 min) with standard C-PC having retention peak timing of 1.448 min, 1.233 min and 0.925 min. As a cautious approach, the purified C-PC was further lyophilized to extend its shelf life as compared to its liquid isoform. To evaluate the bioactive potential of the purified C-PC *in silico* approach was attempted. The molecular docking technique was carried out of C-PC as a ligand-protein with free radicals and α -amylase, α -glucosidase, glycogen synthase kinase-3 and glycogen phosphorylase enzymes as receptors to predict the free radical scavenging (antioxidant) and to target antidiabetic property of C-PC. In both receptors free radicals and enzymes, ligand C-PC plays an important role in establishing interactions within the cavity of active sites. These results established the antioxidant potential of C-PC and also give a clue towards its antidiabetic potential warranting further research.

DOI: <http://dx.doi.org/10.14715/cmb/2021.67.4.8>

Copyright: © 2021 by the C.M.B. Association. All rights reserved.



Introduction

Cyanobacteria are microalga that serves to be the primary producer in aquatic ecosystems which in turn are cosmopolitan within the biosphere and exhibit substantial diversification as compared to their auxiliary prokaryotic counterparts (1, 2). These prokaryotes are predominantly constituted by C-phycoyanin (C-PC), a photosynthetic pigment responsible for imparting their characteristic blue color (3). Cyanobacterial biomass as well as bioactive

products derived from it have been analyzed and well documented in pharmaceuticals, cosmeceuticals, nutraceuticals, health supplements, aquaculture, bioremediation, bioenergy, biofuels and the food industry (4-7).

For a long, researchers have been attracted by the *Plectonema* sp., a filamentous cyanobacterium that is non-toxic and non-heterocystous in nature. Its fast doubling time of approximately 60 hours and minimal requirement for nitrogen sources and light has made it

*Corresponding author. E-mail: alvinafarooqui@yahoo.co.in; ahmadsaheem@gmail.com

an important experimental candidate (8-10). *Plectonema* sp. possesses a great variety of pigments namely carotenoids, chlorophyll and phycobiliproteins (PBP) (11). Among all these members, carotenoids are usually considered to be essential and are structurally related to isoprenoid molecules. The carotenoids are often referred to as pigments owing to their light-absorbing properties (12). Chlorophyll within *Plectonema* sp. plays an additional chelating role which in turn is pivotal for cell repair, increases hemoglobin in the blood, fastens cell growth, aids liver cirrhosis cure an ulcer in humans (13).

PBP is a group of pigmented proteins present in blue-green algae (cyanobacteria) and also in cryptomonads, red algae, etc (14). Generally, PBPs are mainly classified into three types, such as C-phycoerythrin (C-PE), C-phycoerythrin (C-PC) and C-allophycocyanin (C-APC) (15, 16). PBPs differ in their spectral properties and are classified based on absorption spectra: C-PE (Red; λ max = 540 – 570 nm), C-APC (Blue with a green signal; λ max = 650 – 655 nm) and C-PC (Brilliant blue; λ max = 610 – 620 nm) (17). PBPs are hydrophilic and stable fluorescent proteins, having high concentrations resulting in the bluish appearance of the organism and participate in energy transfer processes during photosynthesis (18). The fluorescent nature of PBP is exploited in many fields such as research, diagnostics and therapeutics (19, 20). In PBP, the two subunits α and β polypeptide chains are present in equal amounts (21). Subunit α has a low molecular weight (MW) of 12 – 19 kDa while β is 14 – 21 kDa. These subunits can assemble in various combinations of the trimer ($(\alpha\beta)_3$) (about 120 kDa) or hexamer ($(\alpha\beta)_6$) (about 240 kDa) forms (22, 23).

Commercially, C-PC is a highly important natural product with potential biotechnological applications in cosmetics, food, biotechnology, medicine and pharmacology (24). C-PC as non-carcinogenic and non-toxic natural food colourants are gaining remarkable prominence in view of synthetic food colorants, furthermore, their therapeutic value has also been proven (25, 26). Based upon differential purity ratio levels C-PC is classified as reactive grade (0.7), food grade (3.9) and analytical grade (ratio > 4) (27).

Diabetes mellitus is a major metabolic syndrome characterized by high blood glucose levels caused due to enhance the production of hepatic glucose,

pancreatic impaired insulin production, and insulin resistance (28). Several endogenous and exogenous factors are attributed to the pathogenesis of diabetes mellitus. As an endogenous factor, oxidative stress is considered an important determinant of type 2 diabetes mellitus (29). Overproduction of free radicals such as hydroxyl radicals, superoxide radicals, hydrogen peroxide and nitric oxide radicals creates an imbalance between antioxidants inside the body resulting in oxidative stress (30, 31). On the other hand, blood sugar levels are severely regulated by the action of several enzymes such as α -amylase, α -glucosidase, glycogen synthase kinase-3 and glycogen phosphorylase. α -amylase is responsible for breaking down long-chain carbohydrates (32), while α -glucosidase directly converts carbohydrates into glucose in the small intestine. Glycogen synthase kinase-3 (GSK-3) is a serine/threonine kinase implicated in the development of insulin resistance, mainly based on its role in the regulation of glycogen synthesis (33). Whereas, glycogen phosphorylase (GP) catalyzes the breakdown of glycogen to glucose-1-phosphate in the liver and tissue to generate metabolic energy. In the liver, glucose-1-phosphate is frequently converted by phosphoglucomutase and glucose-6-phosphatase to glucose, which is released for the benefit of other tissues (34). The inhibition of α -amylase, α -glucosidase, GSK-3 and GP and free radical can be recognized as a therapeutic target for the control of type 2 diabetes.

Many synthetic drugs are available as an antioxidant and for the treatment of diabetes, although these are fraught with side effects (35). Therefore, recent research is directed towards treatments using natural materials that have fewer side effects (36). Cyanobacterial bioactive compounds have nowadays become an attractive source of functional compounds, including antioxidants and antidiabetic therapeutic agents. C-PC the most dominant pigment-protein complex of cyanobacteria has also been analyzed and documented in pharmaceuticals, cosmeceuticals, nutraceuticals, health supplements and biomedical research (14). As represented in our previous study, eight cyanobacterial strains were screened to evaluate the maximum crude C-PC producing strain. *Plectonema* sp. was found to be the superior producer of C-PC (37) and thus this strain has been used further for purification and characterization of C-PC. Despite

such inherent potential of *Plectonema* sp. there exist paucity in the elucidation of optimum purification and characterization of C-PC from the same. C-PC is commonly extracted by freeze-thawing, concentrated by ammonium sulphate fractionation, purified by ion-exchange chromatography and more stabilized by lyophilization/freeze-dry method and characterized by Ultraviolet-visible spectroscopy (UV-vis), Fluorescence Spectroscopy, Fourier Transform Infrared (FT-IR) Spectroscopy, Circular Dichroism (CD) Spectroscopy and Sodium Dodecyl Sulphate-Polyacrylamide Gel Electrophoresis (SDS-PAGE) and High-performance liquid chromatography (HPLC). In light of these critical techniques, in the present study, we tried to optimize the standard critical conditions such as differential extraction processes and their after-effects on downstream processing procedures critically mediating C-PC yield and quality from *Plectonema* sp. Further, we investigated the free radical scavenging (antioxidant) and antidiabetic potential of ligand C-PC through molecular docking techniques by inhibiting targeted free radicals and enzymes.

Materials and methods

Materials

Dialysis membrane (3.5 kDa), dipotassium hydrogen phosphate (K_2HPO_4), potassium dihydrogen phosphate (KH_2PO_4), methanol, glacial acetic acid, sodium chloride (NaCl), sodium hydroxide (NaOH), ammonium persulphate (APS), bis-acrylamide, glycerol and TEMED (N, N, N, N-tetramethylethylenediamine) were purchased from Hi-Media. Sodium dodecyl sulfate (SDS) and coomassie blue dye were obtained from G-Biosciences, whereas bromophenol blue and glycerol were purchased from Rankem. A pre-stained protein marker was obtained from PUREGENE and trichloroacetic acid was purchased from Fisher Scientific. Diethylaminoethyl-cellulose (DEAE-C) column matrix, ethidium bromide, EDTA and acetonitrile were purchased from Sigma-Aldrich and, glycine and acrylamide were obtained from Merck. Analytical-grade chemicals were used in this study.

Methods

Experimental Cyanobacterium

Plectonema sp. used during the present study was generously provided by Dr. S. M. Prasad, Department of Botany, University of Allahabad.

Culture Maintenance

Cyanobacterial culture (*Plectonema* sp.) was cultured under standard conditions (Temperature = 27 ± 2 °C). For regular experiments slightly modified BG-11 medium was utilized as described in our previous study, including 14/10 hrs of light and dark photoperiod respectively; pH = 7.0 along with 2400 Lux of light intensity (37-39).

Crude Extraction and Spectrophotometric Estimation of C-PC

Approximately two-week log phase culture was homogenized and centrifuged (5,000 rpm, 10 minutes, 4 °C). Finally, the resultant pellet was washed using phosphate buffer (10 mM; pH 7.4) having 50 mM NaCl and 0.002 M sodium azide (NaN_3) (40). The pellet was again resuspended in the same buffer with the addition of fine glass powder and then frozen at -20 °C. Repeated freeze-thawing of tubes containing pellets was done to accumulate phycobiliproteins in phosphate buffer. After freeze-thaw, crude C-PC was obtained as blue supernatant by centrifugation at 12,000 rpm for 15 minutes at 4 °C. To prevent denaturation of C-PC, 1 μ l / ml of PMSF (Phenyl methyl sulphonyl Fluoride) (100 μ g/ml) was added (41).

Estimation of the amount of C-PC and purity were determined as described by (42, 43).

$$C_{C-PC} = \frac{A(620) - 0.474 A(652)}{5.34}$$

Where C_{C-PC} is the concentration of C-PC in μ g/ml, A (620) is the absorbance of the sample at 620 nm and A (652) is the absorbance at 652 nm.

$$\text{Purity} = A_{620}/A_{280}$$

Where A_{620} is representative of the maximum C-PC absorber peak and A_{280} is an indication of undesired protein especially aromatic amino acids.

Purification of Crude C-PC

Ammonium Precipitation

C-PC crude extracts were separated through gradual precipitation by ammonium salts up to 60 % saturation. The sample was further left undisturbed overnight (4 °C). The precipitate was further

harvested by centrifugation (10,000 rpm; 10 minutes; 4 °C temperature). The resulting supernatant (clear) was discarded and a blue pellet was collected containing C-PC (44).

Dialysis

To increase the level of purity of C-PC, dialysis was performed by suspending ammonium sulfate precipitated pellets in PBS (10 mM; pH = 7.4). The dialysis membrane (3.5 kDa, Himedia) was pretreated to remove membrane-bound contaminants as previously described (45). Briefly, the resuspended sample was subjected to dialysis in 100 – 200 folds of a volume of PBS (10 mM; pH = 7.4).

Ion Exchange Chromatography

The dialysed C-PC was subjected to ion-exchange chromatography to increase its purity by employing DEAE cellulose-packed columns. Dialysed C-PC binds this positive charge matrix and was thus purified according to the procedure described by (46). After incubation of dialysed C-PC with that DEAE-C column at 4 °C was briefly cleaned using appropriate buffer (10 mM; pH = 7.4) to eliminate undesirable C-PC proteins. Nearly different fractions of C-PC were subjected to UV-vis spectrophotometer for their absorbance in the range of 250 – 750 nm (Eppendorf BioSpectrometer, Germany) and their absorption were specifically recorded at wavelengths i.e. 280, 562, 620 and 652 nm.

Characterization of Purified C-PC

UV-visible Spectroscopy

Absorbance spectra of purified and standard C-PC were recorded in the range of 250 – 750 nm using a UV-vis spectrophotometer (Eppendorf Biospectrometer, Germany). The purity of C-PC was calculated as stated above in section 2.2.3.

Fluorescence Spectroscopy

Fluorescence emission spectra of commercially available as a standard and all stages of purified C-PC samples were recorded in the range 290 – 450 nm. C-PC samples were excited at 280 nm and emissions were recorded at 350 nm on Agilent carry eclipse fluorescence spectrophotometer. Fluorescence emission at 350 nm confirmed that the purified sample was the protein that was C-PC (47).

Fourier Transform Infrared Spectroscopy (FT-IR)

Transmission profiles of available standard and all stages purified C-PC were recorded at 450 – 4000 cm^{-1} on a spectrum FT-IR spectrometer (Perkin Elmer, Inc., USA) (48).

Circular Dichroism (CD)

CD spectra of standard, ammonium precipitated, dialysed and column purified C-PC were recorded as per the protocol described by (49). Briefly, different extracts were placed in a temperature-controlled cell holder (25 °C) enclosed with a water bath (Neslab's RTE 110). All the samples were evaluated at a wavelength ranging from 190 to 250 nm (scan speed 20 nm per minute).

Sodium Dodecyl Sulphate-Polyacrylamide Gel Electrophoresis (SDS-PAGE) Analysis

Purified cyanobacterial protein was qualitatively evaluated using SDS-PAGE for their molecular weight according to the previously described protocol (50). To confirm the purity of C-PC, 12 % SDS-PAGE was performed under non-denaturing conditions. The bands were visualized by Coomassie blue staining. The molecular weight of the purified C-PC was determined by running a pre-stained protein marker (PUREGENE) along with the sample (51).

High-Performance Liquid Chromatography (HPLC)

Standard and extracted column purified C-PC samples were further characterized using HPLC (51). C-18 reverse phase column was used during HPLC analysis (Shimadzu-LC-20AD, Japan). Prior to an assessment, 20% acetonitrile with 0.1% trichloroacetic acid was used to equilibrate the C-18 reverse-phase column.

Freeze-Drying: Stepwise Process

The column eluted C-PC protein obtained was in a dilute state and further characterization, assays for its bioactive properties due to its low concentration were inconceivable, which instigated us to find a way to concentrate the obtained protein samples.

The best available and economical method to solve this problem was to perform lyophilization or freeze-drying of C-PC proteins. Briefly, the protein samples

were allowed to freeze at -80°C for 12 hours. The frozen samples were then attached to the freeze-drying vacuum nozzle in the freeze dryer flask and the freeze dryer was switched on. A temperature of -40°C was maintained in the cooling well and with a negative pressure of 50 mTorr and left for $\sim 20 - 24$ hours to complete a cycle.

Molecular docking study

Molecular Docking Analysis of C-PC and Free Radicals

The 3-dimensional (3D) structure of C-PC as a ligand for scavenging and antidiabetic agent were taken from the protein data bank (PDB) with PDB ID: 4L1E [Figure 1 (A)] for the docking study. Protein was prepared by deleting water, ligands and all the chains except A chain. The targeted structures of hydroxyl radical (CID: 961), superoxide radical (CID: [5359597](#)), hydrogen peroxide (CID: 784), and nitric oxide radical (CID: [145068](#)) was obtained from the PubChem database. The MMFF94 force field was used for the energy minimization of the target molecule. Gasteiger partial charges were added, non-polar hydrogen atoms were merged, and rotatable bonds were defined. Docking calculation was carried out on the protein molecule. Essential hydrogen atoms, Kollman united atom type charges, and salvation parameters were added with the aid of AutoDock tools. Grid maps of $60 \times 60 \times 60 \text{ \AA}^3$ grid points were generated with the help of the Auto grid program. C-PC was embedded in a 3D grid, and a probe atom was placed at each grid point. AutoDock parameter set and the distance-dependent dielectric functions were used in the calculation of the Van der Waals and the electrostatic terms, respectively. The torsion of the ligand molecule was set randomly. Each docking experiment was derived from 10 different runs that were set to terminate after a maximum of 2,500,000 energy evaluations. The population size was set to 150. The final [Figure 1 (B)] was generated with the help of Discovery Studio Visualizer (Accelrys) (30, 52).

Molecular Docking Analysis of C-PC and Enzymes

Protein-protein molecular docking was performed via the ZDOCK technique to figure out the protein-protein association between C-PC as a ligand-protein molecule and α -amylase, α -glucosidase, GSK-3 β and

GP as targeted protein molecules. C-PC (PDB ID: 4L1E) structures were obtained from PDB. α -amylase (PDB ID: 4W93), α -glucosidase (PDB ID: 3WY1), GSK-3 β (PDB ID: 3F7Z) and GP (PDB ID: 1L5Q) structures were obtained from PDB. ZDOCK is one of the most unbeaten suites that encompass large calculation facilities in Critical Assessment of Predicted Interactions (CAPRI) (53). ZDOCK is an original phase rigid body molecular docking algorithm that utilizes a fast Fourier transform (FFT) calculation to calculate progress performance for translational searching (54, 55).

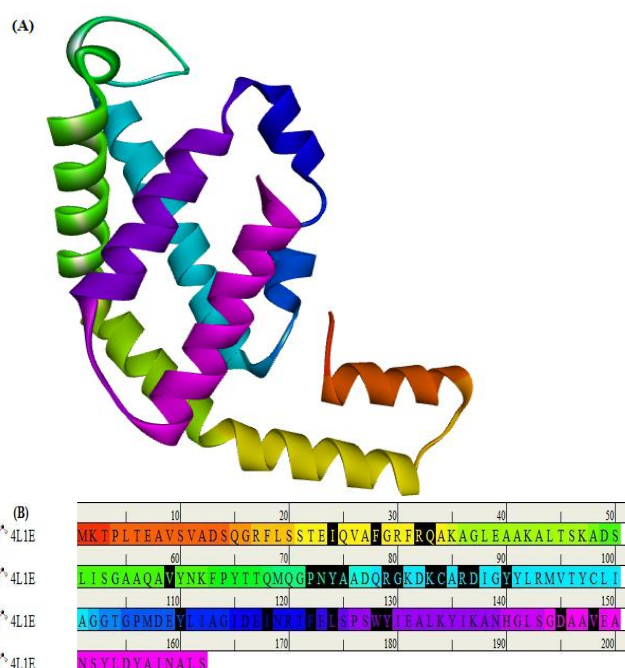


Figure 1. (A) Crystal structure of 'A' chain of C-PC, image from PDB (PDB ID: 4L1E), (B) Amino acid sequence of 'A' chain of C-PC, black highlighted amino acid sequence represents active sites of C-PC and images were generated from Biovia Discovery studio.

Statistical Analysis

The data were represented as mean \pm standard deviation (SD). Statistical significance of the results was determined by using one-way ANOVA followed by Tukey post-test using graph pad Prism (version 5.01), where ns = non-significant, * $p < 0.05$, ** $p < 0.01$ and *** $p < 0.001$ were considered as significant.

Results and discussion

Crude Extraction and Estimation of C-PC

The purity ratio of the C-PC was obtained at different steps of purification by ammonium sulphate

precipitation, dialysis and ion-exchange chromatography on the DEAE cellulose column. The purity ratio (A_{620} / A_{280}) showed a regular increase at each purification step. The initial crude extract showed a purity ratio (A_{620} / A_{280}) of 1.81. C-PC was eluted with a linear gradient of phosphate buffer (25 – 100 mM). Column chromatography of the 100 mM fraction gave the high purity ratio ($A_{620} / A_{280} = 4.12$) as compared to standard ($A_{620} / A_{280} = 4.47$) (Figure 2).

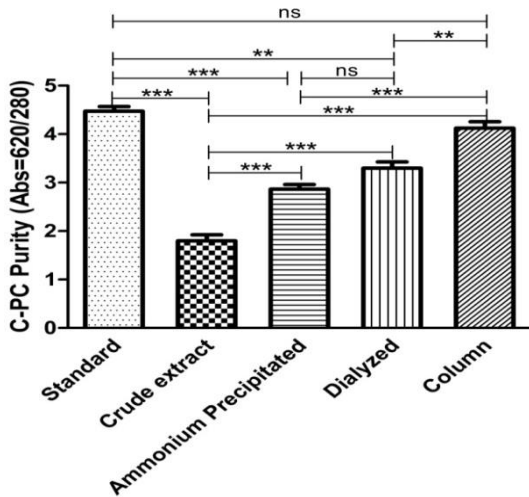


Figure 2. The purity of C-PC at different steps of purification and level of significance. The data are mean \pm SD of three independent experiments, where, ns = non-significant, ** $p < 0.01$ and *** $p < 0.001$.

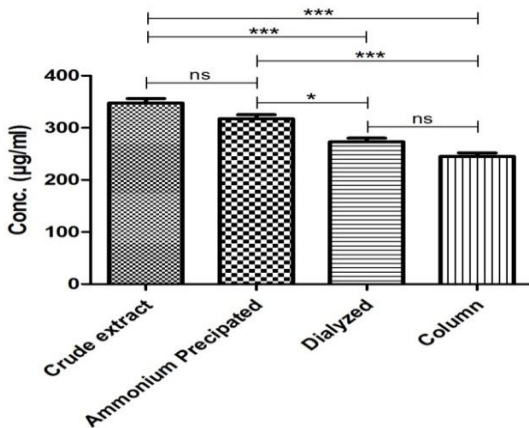


Figure 3. The yield of C-PC in various stages of the purification from *Plectonema* sp. The data are mean \pm SD of three independent experiments, where, ns = non-significant, * $p < 0.05$ and *** $p < 0.001$.

Results presented in Figures 2 and 3 demonstrate the yield and purity of the C-PC respectively obtained at each step of purification. The purity of C-PC in the initial extract was very low. Further increase in the purity from 1.81 to 4.12 was found successively by

following the method of purification with a simultaneous decrease in the yield of the C-PC from 347.67 $\mu\text{g} / \text{ml}$ to 245 $\mu\text{g} / \text{ml}$. The impurity of C-PC protein decreased in terms of recovery at the initial extract crude step to the final chromatography step was $99.6 \pm 3.7 \%$ and $57.2 \pm 3.5 \%$ respectively.

Characterization of Purified C-PC

UV-visible Spectroscopy

The absorption characteristics spectrum of standard, crude, ammonium precipitated dialyzed and column purified C-PC obtained from *Plectonema* sp. was recorded from 250 to 750 nm as represented in Figure 4. A sharp peak at 620 nm suggested high C-PC present in test samples at various stages of purification. The steepest peak was seen in the column purified phase of C-PC. No absorption peak at 650 nm or 540 nm was detected, confirming the absence of C-phycoerythrin and C-allophycocyanin in the sample.

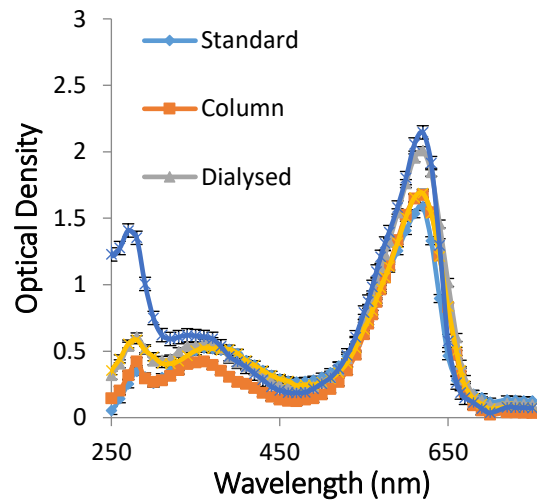


Figure 4. UV-vis spectroscopy graph of standard, crude, ammonium precipitated, dialysed and column purified C-PC. The data are mean \pm SD of three independent experiments.

Fluorescence Spectroscopy

A sharp peak in standard C-PC near 350 nm was observed which is specific for tryptophan residues, suggesting that the protein is in its folded form. All samples of C-PC exhibit a peak near 350 nm while the most prominent peak was observed in column purified extracts of C-PC indicating the pure form of C-PC (Figure 5).

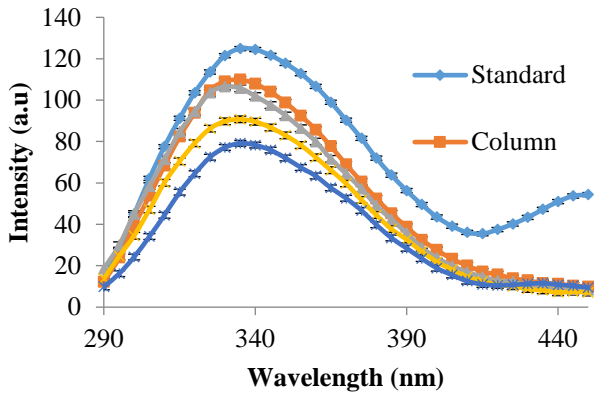


Figure 5. Fluorescence spectroscopy graph of standard, crude, ammonium precipitated, dialysed and column purified C-PC. The data are mean \pm SD of three independent experiments.

Fourier Transform Infrared Spectroscopy (FT-IR)

Amides I is the major band in the protein IR spectrum in the region between $\sim 1600 - 1700 \text{ cm}^{-1}$. Fourier transform infrared spectra (FT-IR spectra) of standard, crude, ammonium precipitated, dialysed and column purified extract of C-PC of *Plectonema* sp. exhibited the protein-specific amide I band at 1637, 1636, 1637, 1636, 1638 cm^{-1} (C=O stretching) (Figure 6). The position and shape of the amide I bands are used for the analysis of the secondary structure of the protein. The sharp band of amide I for C-PC represents the α -helix as the main component of its secondary structure. Simultaneously, the IR spectra of C-PC ensure its purity by the absence of inorganic sulfates and phosphates (representing intensive bands at 1043 and 1015 cm^{-1}).

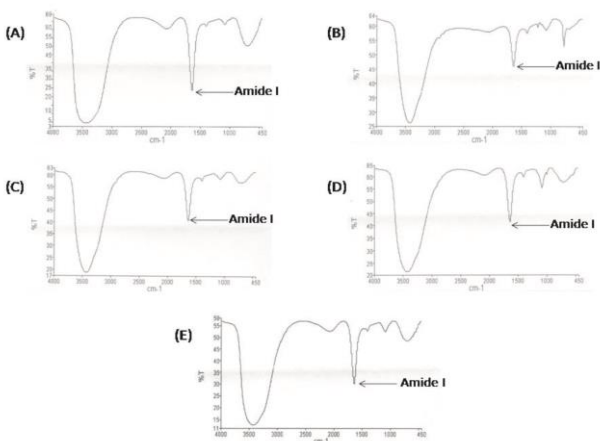


Figure 6. FT-IR spectroscopic graphs of (A) standard, (B) crude, (C) Ammonium precipitated (D) Dialysed and (E) Column chromatography eluted C-PC. 3.2.4. Circular Dichroism (CD)

The CD spectra of all the C-PC samples showed two minima at 208 and 222 nm, a feature of α -helix structure proteins, which are in accordance with the CD spectra of standard C-PC (Figure 7). Similarities in the relative proportions of secondary structure in all C-PC samples suggest the purity of the isolated C-PC. To better assess the structural transition, the CD spectra of C-PC were de-convoluted through the K2D3 software. The α -helix content in standard C-PC was 80.59 % while ammonium precipitated, dialysed and column purified extract of C-PC exhibited 84.59 % α -helix content.

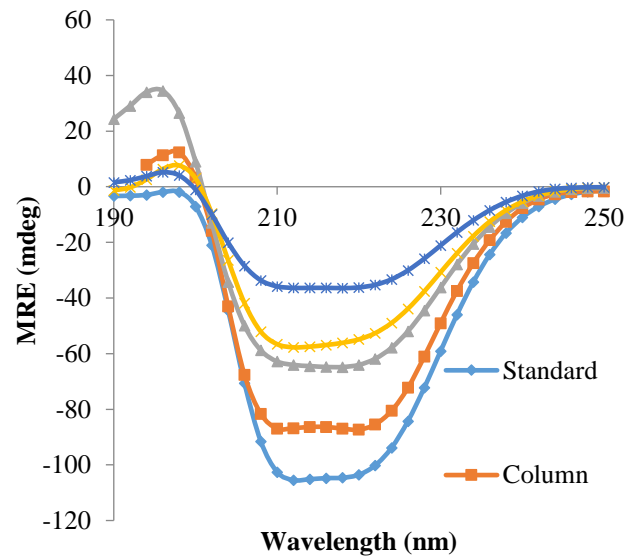


Figure 7. Graphs of circular dichroism of standard, crude, ammonium precipitated, dialysed and column purified C-PC.

Sodium Dodecyl Sulphate-Polyacrylamide Gel Electrophoresis (SDS-PAGE)

The purity of purified C-PC was analysed by 12 % SDS-PAGE (lane-1 crude extraction, lane-2 high-intensity standard, lane-3 ammonium precipitated, lane-4 dialysed and lane-5 ion-exchanged column chromatography samples respectively). The SDS-PAGE analysis of all purified C-PC showed two main bands corresponds to α and β subunits of C-PC, further validating its homogeneity and purity by comparing with standard C-PC (lane-2). Additionally, the calculated molecular mass of α and β subunit was found to be 17 kDa and 19 kDa (Figure 8).

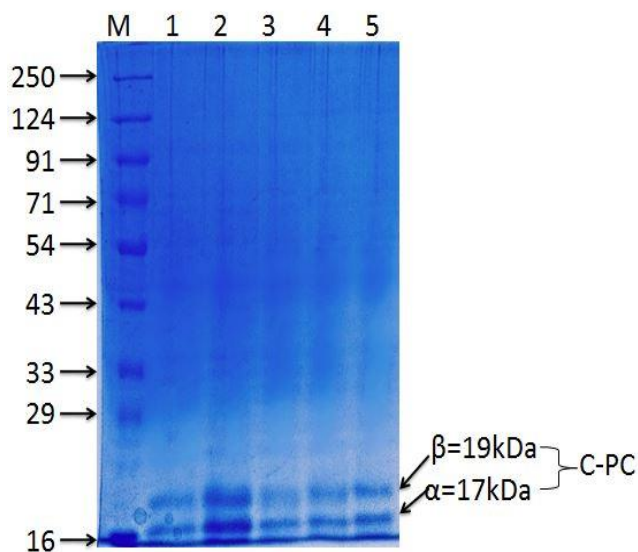


Figure 8. 12% SDS-PAGE analysis of purified C-PC from *Plectonema* sp., M- Protein molecular marker; 1- Crude extract; 2- Standard; 3- Ammonium sulphate precipitated; 4- Dialysed and 5- Ion-exchange column chromatography.

High-performance liquid chromatography (HPLC)

HPLC analysis of standard C-PC and purified column C-PC was performed at 620 nm. Purified column C-PC of *Plectonema* sp., showed peaks with the retention time of 1.465 min, 1.234 min, 1.097 min and 0.905 min, equivalent to the standard peak at 1.448 min, 1.233 min and 0.925 min. [Figure 9 (A) and (B)] confirming the identity of the sample as C-PC.

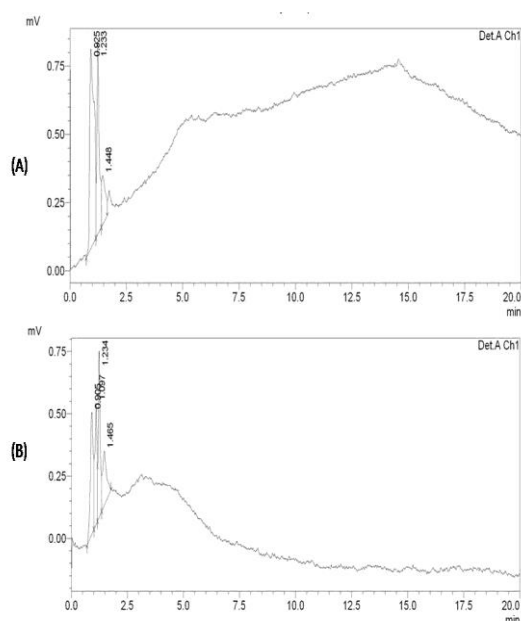


Figure 9. HPLC chromatogram of (A) standard C-PC and (B) purified column C-PC from *Plectonema* sp.

Molecular Docking Analysis of C-PC with Free Radicals

The docked complex of C-PC ligand molecule with targeted molecule hydroxyl radical showed that the complex was formed by the hydrogen bond interaction of targeted molecule hydroxyl radical with ARG30 and SER37 residues of C-PC. The hydrophobic interaction was observed between targeted molecule hydroxyl radical and GLY102 and ARG30 residues of C-PC [Figure 10 (A)], the docked complex had binding energy (ΔG) of -2.5 kcal/mol.

The docked complex of C-PC ligand with targeted molecule superoxide radical was formed by a hydrogen bond between superoxide radicals and LYS1 residue of C-PC, hydrophobic interaction was observed between targeted superoxide radical and GLY105 residue of C-PC [Figure 10 (B)], the binding energy was -2.19 kcal/mol. In the docked complex of C-PC and hydrogen peroxide, hydrogen bonds and hydrophobic interaction were found between hydrogen peroxide THR104 residue of C-PC [Figure 10 (C)], the binding energy was -2.24 kcal/mol.

The docked complex of C-PC with nitric oxide radical was formed by the hydrogen bond and hydrophobic interaction between nitric oxide radical and TYR129 residue of C-PC [Figure 10 (D)], the binding energy was found to be -3.44 kcal/mol (Table 1). Complexes with the highest binding were selected for analyzing the stability of protein-target interaction.

Table 1. Binding Energy, Intermolecular Energy, Inhibitory Constant, Binding residues and Hydrogen bonds length comparison table of C-PC with free radicals molecular docking; target (A), Binding Energy (kcal/mol) (B), Intermolecular Energy (kcal/mol) (C), Inhibitory Constant (mM) (D), Binding residues (E), Hydrogen bonds length (Å) (F)

A	B	C	D	E	F
Hydroxyl radical	-2.5	-2.5	14.52	ARG30, SER37	2.8, 3.12
Superoxide radical	-2.19	-2.19	24.67	LYS1	2.9
Hydrogen per oxide	-2.24	-2.38	28.54	THR104	2.7
Nitric oxide radical	-3.44	-3.72	2.99	TYR129	2.7

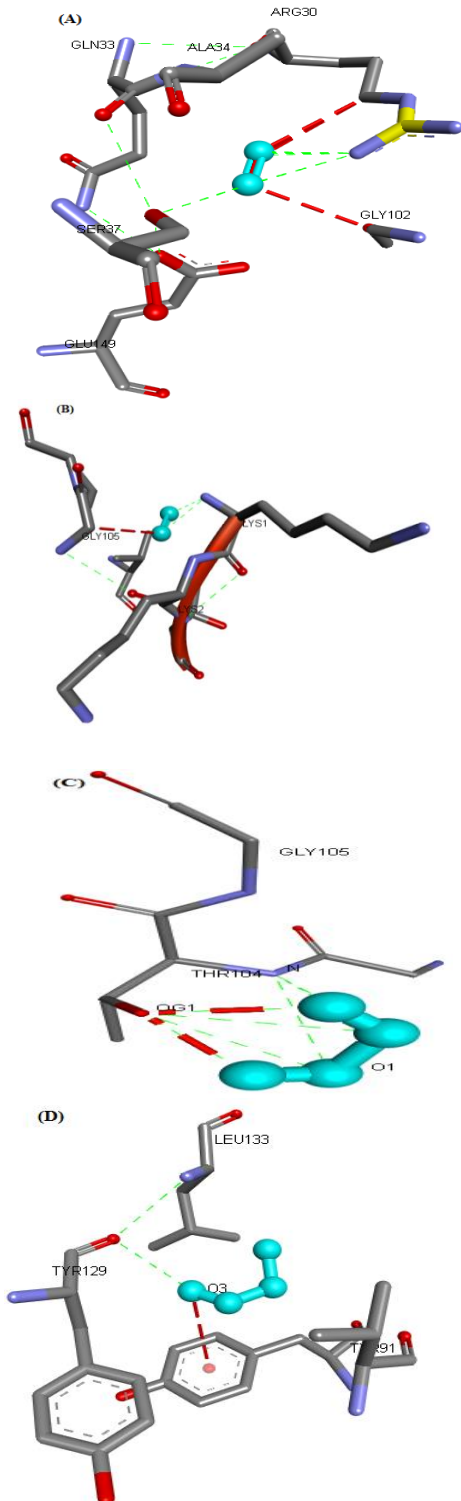
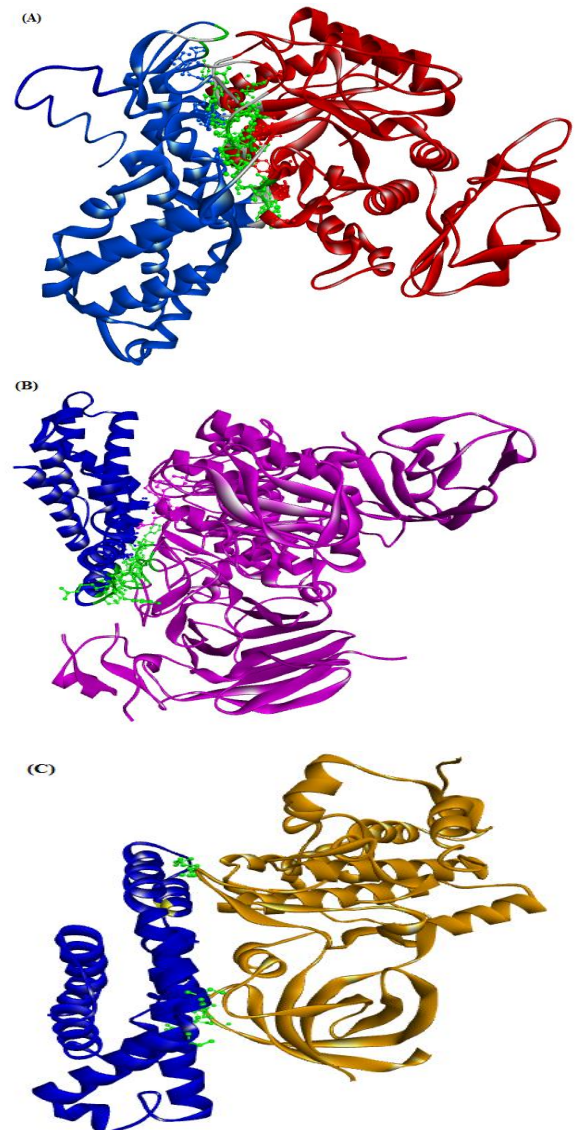


Figure 10. Molecular docking interaction of C-PC with free radical. C-PC (Ligand) is represented in sticks and free radical (Target) is represented in stick and ball form, hydrogen bonds are represented in green colour, hydrophobic interactions are represented in red colour, (A) Molecular docked model of C-PC with hydroxyl radical, (B) Molecular docked model of C-PC with superoxide radical, (C) Molecular docked model of C-PC with hydrogen peroxide and (D) Molecular docked model of C-PC with nitric oxide radical.

Molecular Docking Analysis of C-PC with Enzymes

The ZDOCK generated the top 10 docked predictions. All of the complexes were evaluated using the ZDOCK score. ZDOCK Score (force field) = $-(\text{ligand/receptor interaction energy} + \text{ligand internal energy})$ (Xiong et al., 2013). Complexes with the highest ZDOCK scores were selected for analyzing the stability of protein-protein interaction. The ZDOCK score for the interaction of C-PC with the residue of α -amylase and α -glucosidase interaction was found to be 1588.66 and 1823.19 respectively. The ZDOCK score of the C-PC with GSK-3 β and GP was found to be 1525.48 and 1794.53, respectively (Figure 11).



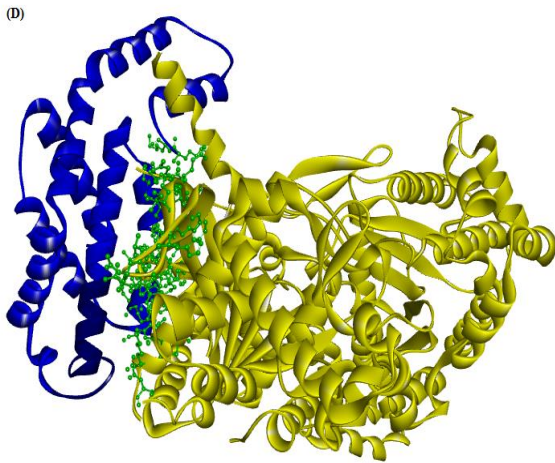


Figure 11. Visualization of best docking complexes of the interaction of C-PC with α -amylase, α -glucosidase, GSK-3 β and GP generated by ZDOCK with highest Z-score. C-PC is represented as solid ribbon (blue colored), interacting residues are represented as ball and stick (green colored), (A) Interaction of C-PC with α -amylase (red-colored solid ribbons), (B) Interaction of C-PC with α -glucosidase (purple colored solid ribbons), (C) Interaction of C-PC with GSK-3 β (orange-colored solid ribbons) and (D) Interaction of C-PC with GP (yellow-colored solid ribbons).

Cyanobacterial phycobiliproteins have gained importance due to their potential applications in different commercially important sectors. One such phycobiliprotein is C-PC which beholds numerous applications and is isolated, purified and characterized from *Plectonema* sp. (56). Different purification procedures affect C-PC concentration because the efficiency of one procedure on particular *Plectonema* sp. may not be efficient for the others. To overcome this drawback our study was designed to elucidate a broad applicable C-PC isolation and purification method for *Plectonema* sp. The four major steps employed for the isolation and purification of C-PC from *Plectonema* sp. were (i) crude extract preparation, (ii) ammonium sulfate precipitation, (iii) dialysis, and (iv) anion exchange chromatography. The competence of extraction methods was determined by calculating the concentration and purity ratio of isolated C-PC. The purity of C-PC plays a considerable role in commercial applications (56) and is generally estimated using the absorbance ratio of A₆₂₀/A₂₈₀ (57). The purity of C-PC after ammonium sulphate precipitation was found to be 1.81 folds enhanced in comparison to the crude extract having a concentration of 347.67 μ g/ml with an initial recovery

of 99.6%. Moreover, the dialysis of ammonium sulphate precipitated fraction further augmented its purity content by 1.5 folds having a concentration of 317 μ g/ml and a decreased recovery of 86.5%. This step is predominantly useful in salting-out unwanted proteins simultaneously concentrating C-PC. Furthermore, C-PC was finally purified by DEAE Cellulose column, which further increased the purity level by 1.25 folds as compared to dialyzed C-PC having a concentration of 245 μ g/ml with further decreased recovery of 57.2%. The highest purity ratio of 4.12 at the final purification step of column chromatography was also found to be nearly equivalent to the purity ratio of a standard that is 4.47.

The absorption spectra of the column purified C-PC exhibited a prominent peak at 620 nm which was in accordance with the peak of standard C-PC. Additionally, the C-PC of *Plectonema* sp. was further characterized for its intrinsic fluorescence properties using fluorescence spectroscopy. The sharp emission peak at 350 nm of column purified C-PC elucidated the presence of C-PC which has been earlier specified for the native form of this protein thereby validating its purity (58). The absence of peaks at 1043 and 1015 cm^{-1} in FT-IR spectra confirms the absence of inorganic impurities, while the sharp amide I band in standard along with column purified C-PC indicates α -helix as the chief constituent of its secondary structure (59). CD spectra of standard and column purified C-PC exhibit two negative minima in the ultraviolet region at 208 nm and 222 nm, which is a characteristic of the α -helical structure of the protein. The two negative peaks both contributed to an $n \rightarrow \pi^*$ transition for the peptide bond with α -helicity (60) demonstrated the α -helical structure of C-PC, devoid of β -sheets. In the array to characterize C-PC, HPLC was performed using C18 reverse-phase column, exhibiting peaks with retention times of 1.465 min, 1.234 min, 1.097 min and 0.909 min. which was, equivalent to the peaks of standard C-PC of 1.448 min, 1.233 min and 0.925 min. Moreover, SDS-PAGE also confirmed the two highly intensified bands from column purified C-PC in comparison with the standard and revealed its α and β subunits with a molecular weight of 17 and 19 kDa respectively, thereby confirming the purity of C-PC.

Oxidative stress through the production of free radicals has been proposed as the root cause of the

development of type 2 DM (61). An antioxidant is known to exert a protective effect against oxidative damage and is linked with a reduced risk of chronic diseases (62). Consequently, molecular docking studies were performed to analyze the association between ligand C-PC and its antioxidant property. C-PC was docked with free radicals; Hydroxyl radicals, superoxide radicals, hydrogen peroxide and nitric oxide radicals using AutoDock 4.2. Molecular docking analysis between C-PC and free radicals demonstrated that C-PC binds with all four free radicals. Our results were in accordance with previous findings of *in vitro* antioxidant activity of C-PC (63). C-PC was found to possess greater interaction (binding energy = -3.44 kcal/mol) with nitric oxide radical as compared to hydroxyl radical (binding energy = -2.5 kcal/mol), superoxide radical (binding energy = -2.19 kcal/mol), hydrogen peroxide (binding energy = -2.24 kcal/mol). These results demonstrate that C-PC is an efficient scavenger of free radicals; therefore, the therapeutic use of C-PC as a natural antioxidant appears promising.

Highly involved mechanisms for antidiabetic therapy are inhibition of intestinal alpha-amylase and alpha-glucosidase, altering the activity of GSK3 and glycogen phosphorylase (64). Alpha-amylase and alpha-glucosidase are the essential enzymes that catalyses the primary step in hydrolysis of starch to maltose and finally glucose. Inhibition of these enzymes in intestine results in delayed carbohydrates digestion (65). GSK3 negatively regulates numerous features of insulin signaling (66) while GP is a significant therapeutic target for type 2 diabetes with a direct effect on blood sugar levels via the glycogenolysis pathway (67). Similar *in vitro* alpha-amylase and alpha-glucosidase inhibition activity were recorded by (68), who investigated the alpha-amylase and alpha-glucosidase inhibition activity was recorded in concentration-dependent manner with increasing concentration of C-PC. Similarly, (69) investigated the *in vitro* antidiabetic activity of purified pigments from three cyanobacterial species; *Microcoleus*, *Lyngbya*, and *Synechocystis* and found that purified C-PC and C-phycoerythrin from all species inhibited the enzyme the most (96.62 %), while crude solvent extracted compounds had the least activity. Hence, to elucidate the antidiabetic potential of the C-PC molecular docking technique was

performed. Z-dock technique of protein-protein interactions was executed between C-PC and enzymes (70). All enzymes bind significantly with C-PC, the docking conformations of C-PC with alpha-amylase, alpha-glucosidase, GSK-3 β and GP deciphering the inhibitory potential of C-PC on enzymes. Our findings were in accordance with an *in silico* study conducted by (71-73), which demonstrated that C-PC inhibits alpha-amylase and alpha-glucosidase by binding to the active site and disrupting substrate-enzyme interactions. The highest ZDOCK score reveals the highest protein-protein interaction. The maximum ZDOCK score was observed by the interaction of C-PC and alpha-glucosidase (ZDOCK score: 1823.19), while the ZDOCK score of interaction C-PC with alpha-amylase, GSK-3 β and GP was found to be 1588.66, 1525.48 and 1794.53 respectively.

Conclusion

Apart from establishing C-PC purification through sequential usage of ammonium sulphate and ion-exchange chromatography, the present study provides an insight for augmenting the relative stability of purified C-PC using lyophilization. Characterization of purified C-PC by various techniques as demonstrated in this study would certainly aid in studies dedicated to the improvement in the stability and the purity of C-PC. The molecular docking outcomes recommend substantial antioxidant and antidiabetic potential of C-PC by interacting with free radicals and enzymes. Furthermore, the *in silico* results not only confirm the findings of the other *in vitro* experiments but also provide light on the overall molecular interaction between C-PC and carbohydrate-metabolism enzymes. To further comprehend the therapeutic potential of C-PC and establish the mechanism of action of C-PC in reducing hyperglycemia in diabetic patients, more scientific validation is required. Indeed, *in silico* screening will play a key role in identifying active ligands for the novel protein targets that are on the horizon.

Conflict of interest

The authors declare that they have no conflicts of interest with the contents of this article.

Acknowledgment

The authors are thankful to the Researchers Supporting Project Number (RSP-2021/86), King Saud University, Riyadh, Saudi Arabia.

References

1. Ganesan V, Raja R, Hemaiswarya S, Carvalho IS, Anand N. Isolation and characterization of two novel plasmids pCYM01 and pCYM02 of *Cylindrospermum stagnale*. *Saudi J. Biol. Sci.* 2020;27(1):535-42.
2. Stucken K, Koch R, Dagan T. Cyanobacterial defense mechanisms against foreign DNA transfer and their impact on genetic engineering. *Biol. Res.* 2013;46(4):373-82.
3. Hu J, Nagarajan D, Zhang Q, Chang JS, Lee DJ. Heterotrophic cultivation of microalgae for pigment production: A review. *Biotechnol. Adv.* 2018;36(1):54-67.
4. Prasanna R, Sood A, Jaiswal P, Nayak S, Gupta V, Chaudhary V, Joshi M, Natarajan C. Rediscovering cyanobacteria as valuable sources of bioactive compounds. *Appl. Biochem. Microbiol.* 2010;46(2):119-34.
5. Abed RM, Dobretsov S, Sudesh K. Applications of cyanobacteria in biotechnology. *J. Appl. Microbiol.* 2009;106(1):1-2.
6. Chu WL. Biotechnological applications of microalgae. *IEJSME.* 2012;6(1):S24-37.
7. Lau NS, Matsui M, Abdullah AA. Cyanobacteria: photoautotrophic microbial factories for the sustainable synthesis of industrial products. *Biomed Res. Int.* 2015;25:2015.
8. Khazi MI, Demirel Z, Dalay MC. Evaluation of growth and phycobiliprotein composition of cyanobacteria isolates cultivated in different nitrogen sources. *J. Appl. Phycol.* 2018;30(3):1513-23.
9. Rigonato J, Alvarenga DO, Fiore MF. Tropical cyanobacteria and their biotechnological applications. In *Diversity and Benefits of Microorganisms from the Tropics 2017* (pp. 139-167). Springer, Cham.
10. Suhail S, Biswas D, Farooqui A, Arif JM, Zeeshan M. Antibacterial and free radical scavenging potential of some cyanobacterial strains and their growth characteristics. *J Chem Pharm Res.* 2011;3(2):472-8.
11. Mandal MK, Chanu NK, Chaurasia N. Cyanobacterial pigments and their fluorescence characteristics: applications in research and industry. In *Advances in cyanobacterial biology.* 2020;(pp. 55-72). Academic Press.
12. Jan S, Abbas N, Jan S, Abbas N. *Chemistry of Himalayan phytochemicals.* Himalayan phytochemicals. Amsterdam: Elsevier. 2018:121-66.
13. Kumar J, Singh D, Tyagi MB, Kumar A. *Cyanobacteria: Applications in biotechnology.* In *Cyanobacteria.* 2019;(pp. 327-346). Academic Press.
14. Manirafasha E, Ndikubwimana T, Zeng X, Lu Y, Jing K. Phycobiliprotein: Potential microalgae derived pharmaceutical and biological reagent. *Biochem. Eng. J.* 2016;109:282-96.
15. Wang A, Yan K, Chu D, Nazer M, Lin NT, Samaranyake E, Chang J. Microalgae as a mainstream food ingredient: demand and supply perspective. In *Microalgae Biotechnology for Food, Health and High Value Products 2020* (pp. 29-79). Springer, Singapore.
16. Sun L, Wang S, Chen L, Gong X. Promising fluorescent probes from phycobiliproteins. *IEEE J. Sel. Top. Quantum Electron.* 2003;9(2):177-88.
17. Pandiraj D, Baldev E, Muhammad Ilyas MH, Thajudin N. Production, extraction and purification of C-phycoerythrin from marine cyanobacterium, *Phormidium persicinum* NTDP01. *Phykos.* 2017;47:16-22.
18. Raja R, Hemaiswarya S, Kumar NA, Sridhar S, Rengasamy R. A perspective on the biotechnological potential of microalgae. *Crit. Rev. Microbiol.* 2008;34(2):77-88.
19. Ge X, Tolosa L, Rao G. Dual-labeled glucose binding protein for ratiometric measurements of glucose. *Anal. Chem.* 2004;76(5):1403-10.
20. Pickup JC, Hussain F, Evans ND, Rolinski OJ, Birch DJ. Fluorescence-based glucose sensors. *Biosens. Bioelectron.* 2005;20(12):2555-65.
21. Bernard C, Thomas JC, Mazel D, Mousseau A, Castets AM, de Marsac NT, Dubacq JP.

- Characterization of the genes encoding phycoerythrin in the red alga *Rhodella violacea*: evidence for a splitting of the rpeB gene by an intron. *Proc. Natl. Acad. Sci.* 1992;89(20):9564-8.
22. De Marsac NT. Phycobiliproteins and phycobilisomes: the early observations. *Photosynth. Res.* 2003;76(1):193-205.
 23. Stadnichuk IN, Tropin IV. Phycobiliproteins: structure, functions and biotechnological applications. *Appl. Biochem. Microbiol.* 2017;53(1):1-0.
 24. Odjadjare EC, Mutanda T, Olaniran AO. Potential biotechnological application of microalgae: a critical review. *Crit. Rev. Biotechnol.* 2017;37(1):37-52.
 25. Moraes CC, Sala L, Cerveira GP, Kalil SJ. C-phycoerythrin extraction from *Spirulina platensis* wet biomass. *Braz. J. Chem. Eng.* 2011;28(1):45-9.
 26. Pandey VD. Cyanobacterial natural products as antimicrobial agents. *Int. J. Curr. Microbiol. Appl. Sci.* 2015;4(1):310-7.
 27. Reis A, Mendes A, Lobo-Fernandes H, Empis JA, Novais JM. Production, extraction and purification of phycobiliproteins from *Nostoc* sp. *Bioresour. Technol.* 1998;66(3):181-7.
 28. Moller DE. New drug targets for type 2 diabetes and the metabolic syndrome. *Nature.* 2001;414(6865):821-7.
 29. Asmat U, Abad K, Ismail K. Diabetes mellitus and oxidative stress—A concise review. *Saudi Pharm. J.* 2016;24(5):547-53.
 30. Khanam A, Ahmad S, Husain A, Rehman S, Farooqui A, Yusuf MA. Glycation and antioxidants: hand in the glove of antiglycation and natural antioxidants. *Curr. Protein Pept. Sci.* 2020;21(9):899-915.
 31. Rao PS, Kalva S, Yerramilli A, Mamidi S. Free radicals and tissue damage: Role of antioxidants. *Free Radic. Antioxid.* 2011;1(4):2-7.
 32. Deuschländer MS, Van de Venter M, Roux S, Louw J, Lall N. Hypoglycaemic activity of four plant extracts traditionally used in South Africa for diabetes. *J. Ethnopharmacol.* 2009;124(3):619-24.
 33. Lin AH, Lee BH, Chang WJ. Small intestine mucosal α -glucosidase: A missing feature of in vitro starch digestibility. *Food Hydrocoll.* 2016;53:163-71.
 34. Henriksen EJ, Dokken BB. Role of glycogen synthase kinase-3 in insulin resistance and type 2 diabetes. *Curr. Drug Targets.* 2006;7(11):1435-41.
 35. Treadway JL, Mendys P, Hoover DJ. Glycogen phosphorylase inhibitors for treatment of type 2 diabetes mellitus. *Expert Opin. Investig. Drugs.* 2001;10(3):439-54.
 36. Grover JK, Yadav S, Vats V. Medicinal plants of India with anti-diabetic potential. *J. Ethnopharmacol.* 2002;81(1):81-100.
 37. Husain, A., Khan, F., Osama, K., Mahfooz, S., Shamim, A., Ahmad, S., & Farooqui, A.. Media optimization for C-phycoerythrin production in *Plectonema* sp. using response surface methodology and central composite design. *Int. J. Res. Pharm. Sci.* 2020;11(3):3897-904.
 38. Mahfooz S, Shamim A, Husain A, Farooqui A. Physicochemical characterisation and ecotoxicological assessment of nano-silver using two cyanobacteria *Nostoc muscorum* and *Plectonema boryanum*. *Int. J. Environ. Sci. Technol.* 2019;16(8):4407-18.
 39. Salama A, Abdel Ghany A, Osman A, Sitohy M. Maximising phycoerythrin extraction from a newly identified Egyptian cyanobacteria strain: *Anabaena oryzae* SOS13. *Int. Food Res. J.* 2015;22(2).
 40. Mahfooz S, Bano S, Shamim A, Husain A, Farooqui A. Partial purification, characterization and bioactive potential of C-phycoerythrin from *Cyanobacterium Plectonema boryanum*. *Biochem. Cell Biol.* 2017;(1):57-64.
 41. Kaur S, Khattar JI, Singh Y, Singh DP, Ahluwalia AS. Extraction, purification and characterisation of phycoerythrin from *Anabaena fertilissima* PUPCCC 410.5: As a natural and food grade stable pigment. *J. Appl. Phycol.* 2019;31(3):1685-96.
 42. Hazra P, Kesh GS. Isolation and purification of phycoerythrin from cyanobacteria of a

- mangrove forest. *Appl. Biol. Chem.* 2017;60(6):631-6.
43. Patil G, Chethana S, Sridevi AS, Raghavarao KS. Method to obtain C-phycoerythrin of high purity. *J. Chromatogr. A.* 2006;1127(1-2):76-81.
 44. Ashraf JM, Shahab U, Tabrez S, Lee EJ, Choi I, Ahmad S. DNA Glycation from 3-Deoxyglucosone Leads to the Formation of AGEs: Potential Role in Cancer Auto-antibodies. *Cell Biochem. Biophys.* 2016 ;74(1):67-77.
 45. Ahmad S, Dixit K, Shahab U, Alam K, Ali A. Genotoxicity and immunogenicity of DNA-advanced glycation end products formed by methylglyoxal and lysine in presence of Cu²⁺. *Biochem. Biophys. Res. Commun.* 2011; 15;407(3):568-74.
 46. Khanam A, Alouffi S, Rehman S, Ansari IA, Shahab U, Ahmad S. An in vitro approach to unveil the structural alterations in d-ribose induced glycated fibrinogen. *J. Biomol. Struct. Dyn.* 2021;39(14):5209-23.
 47. Ahmad S, Shahab U, Baig MH, Khan MS, Khan MS, Srivastava AK, Saeed M. Inhibitory Effect of Metformin and Pyridoxamine in the Formation of Early, Intermediate and Advanced Glycation End-Products. *PLoS ONE.* 2013;8(9).
 48. Rehman S, Faisal M, Alatar AA, Ahmad S. Physico-chemical Changes Induced in the Serum Proteins Immunoglobulin G and Fibrinogen Mediated by Methylglyoxal. *Curr. Protein Pept. Sci.* 2020;21(9):916-23.
 49. Correcirc DH, Ramos CH. The use of circular dichroism spectroscopy to study protein folding, form and function. *Afr. J. Biochem. Res.* 2009;3(5):164-73.
 50. Laemmli UK. Cleavage of structural proteins during the assembly of the head of bacteriophage T4. *Nature.* 1970;227(5259):680-5.
 51. Kumar D, Dhar DW, Pabbi S, Kumar N, Walia S. Extraction and purification of C-phycoerythrin from *Spirulina platensis* (CCC540). *Indian J. Plant Physiol.* 2014;19(2):184-8.
 52. Rizvi SM, Shakil S, Haneef M. A simple click by click protocol to perform docking: AutoDock 4.2 made easy for non-bioinformaticians. *EXCLI J.* 2013;12:831.
 53. Hwang H, Vreven T, Pierce BG, Hung JH, Weng Z. Performance of ZDOCK and ZRANK in CAPRI rounds 13–19. *Proteins: Struct. Funct. Bioinform.* 2010;78(15):3104-10.
 54. Xiong K, Li S, Zhang H, Cui Y, Yu D, Li Y, Sun W, Fu Y, Teng Y, Liu Z, Zhou X. Targeted editing of goat genome with modular-assembly zinc finger nucleases based on activity prediction by computational molecular modeling. *Mol. Biol. Rep.* 2013;40(7):4251-6.
 55. Chowdhury R, Rasheed M, Keidel D, Moussalem M, Olson A, Sanner M, Bajaj C. Protein-protein docking with F2Dock 2.0 and GB-Rerank. *PLoS One.* 2013;8(3):e51307.
 56. Kuddus M, Singh P, Thomas G, Al-Hazimi A. Recent developments in production and biotechnological applications of C-phycoerythrin. *Biomed Res. Int.* 2013;2013.
 57. Pan-utai W, Iamtham S. Physical extraction and extrusion entrapment of C-phycoerythrin from *Arthrospira platensis*. *J. King Saud Univ. Sci.* 2019;31(4):1535-42.
 58. Ghisaidoobe AB, Chung SJ. Intrinsic tryptophan fluorescence in the detection and analysis of proteins: a focus on Förster resonance energy transfer techniques. *Int. J. Mol. Sci.* 2014;15(12):22518-38.
 59. Garidel P, Schott H. Fourier-transform midinfrared spectroscopy for analysis and screening of liquid protein formulations. *Bioprocess Int.* 2006;4(6):48-55.
 60. Kelly SM, Jess TJ, Price NC. How to study proteins by circular dichroism. *Biochim. Biophys. Acta Proteins Proteom.* 2005;1751(2):119-39.
 61. Wright Jr E, Scism-Bacon JL, Glass LC. Oxidative stress in type 2 diabetes: the role of fasting and postprandial glycaemia. *Int. J. Clin. Pract.* 2006;60(3):308-14.
 62. Tan BL, Norhaizan ME, Liew WP, Sulaiman Rahman H. Antioxidant and oxidative stress:

- a mutual interplay in age-related diseases. *Front. Pharmacol.* 2018;9:1162.
63. Romay CH, Gonzalez R, Ledon N, Ramirez D, Rimbau V. C-phycoyanin: a biliprotein with antioxidant, anti-inflammatory and neuroprotective effects. *Curr. Protein Pept. Sci.* 2003;4(3):207-16.
64. Yilmazer-Musa M, Griffith AM, Michels AJ, Schneider E, Frei B. Inhibition of α -amylase and α -glucosidase activity by tea and grape seed extracts and their constituent catechins. *J. Agric. Food Chem.* 2012;60(36):8924.
65. Kajaria D, Ranjana JT, Tripathi YB, Tiwari S. In-vitro α amylase and glycosidase inhibitory effect of ethanolic extract of antiasthmatic drug—Shirishadi. *J. Adv. Pharm. Technol. Res.* 2013;4(4):206.
66. Treadway, J. L., Mendys, P., & Hoover, D. J. (2001). Glycogen phosphorylase inhibitors for treatment of type 2 diabetes mellitus. *Expert Opin. Investig. Drugs.* 10(3), 439-454.
67. Souder, D. C., & Anderson, R. M. (2019). An expanding GSK3 network: implications for aging research. *Geroscience*, 41(4), 369-382.
68. Prabakaran G, Sampathkumar P, Kavisri M, Moovendhan M. Extraction and characterization of phycoyanin from *Spirulina platensis* and evaluation of its anticancer, antidiabetic and antiinflammatory effect. *Int. J. Biol. Macromol.* 2020;153:256-63.
69. Ghosh T, Bhayani K, Paliwal C, Maurya R, Chokshi K, Pancha I, Mishra S. Cyanobacterial pigments as natural anti-hyperglycemic agents: an in vitro study. *Front. Mar. Sci.* 2016;3:146.
70. Maheshwari S, Brylinski M. Predicted binding site information improves model ranking in protein docking using experimental and computer-generated target structures. *BMC Struct. Biol.* 2015;15(1):1-4.
71. Azeez S, Jafar, S., Aziziam, Z., Fang, L., Mawlood, A., Ercisli, M. Insulin-producing cells from bone marrow stem cells versus injectable insulin for the treatment of rats with type I diabetes. *Cell Mol Biomed Rep* 2021; 1(1): 42-51.
72. Kazemi E, Zargooshi J, Kaboudi M, Heidari P, Kahrizi D, Mahaki B, Mohammadian Y, Khazaei H, Ahmed K. A genome-wide association study to identify candidate genes for erectile dysfunction. *Brief Bioinforma* 2021;22(4):bbaa338. <https://doi.org/10.1093/bib/bbaa338>
73. Munawaroh HS, Gumilar GG, Nurjanah F, Yuliani G, Aisyah S, Kurnia D, Wulandari AP, Kurniawan I, Ningrum A, Koyande AK, Show PL. In-vitro molecular docking analysis of microalgae extracted phycoyanin as an anti-diabetic candidate. *Biochem. Eng. J.* 2020;161:107666.